Available online at www.sciencedirect.com
ScienceDirect
Trans. Nonferrous Met. Soc. China 26(2016) 484−491
Transactions of Nonferrous Metals Society of China
www.tnmsc.cn

# Effect of Co content on electrodeposition mechanism and mechanical properties of electrodeposited Ni−Co alloy

M. ZAMANI[1], A. AMADEH[1], S. M. LARI BAGHAL[1,2]

1. School of Metallurgy and Materials Engineering, College of Engineering, University of Tehran, P.O. Box 11155-4563, Tehran, Iran;
2. Department of Materials Science and Engineering, Faculty of Engineering, Shahid Chamran University, Ahvaz 6135785311, Iran

Received 16 February 2015; accepted 6 August 2015

**Abstract:** Ni–Co coatings with various cobalt contents were electrodeposited from modified Watts bath. The effect of cobalt content on electrodeposition mechanism of the coatings was studied by electro-chemical impedance spectroscopy method (EIS). Surface morphology and crystallographic structure of the coatings were investigated by means of SEM and XRD. Mechanical properties of the coatings were determined using Vickers microhardness and tensile tests. It was found that with increasing the $Co^{2+}$ ions in electroplating bath, the charge transfer resistance ($R_{ct}$) of Ni−Co film increased whereas the Warburg impedence decreased. This may be due to enhancement in coverage of cathode surface by $Co(OH)_2$ and higher diffusion rate of metal ions towards cathode surface, respectively. Also, with increasing the cobalt content in the bath, cobalt content in the alloy coating increased anomalously and (111) texture consolidated gradually. With increasing the cobalt content up to 45% in alloy coating, the grain size decreased and consequently, hardness and strength of the alloy increased. Further enhancement of cobalt content up to 55% led to a little decrease in hardness and strength. The maximum ductility was observed for Ni−25%Co coating due to relatively small grain size and compact structure.

**Key words:** Ni−Co coating; electrodeposition; microstructure; mechanical properties

## 1 Introduction

Ni coatings are frequently used as tough and strong material in microsystems, electroforming and anti-wear applications [1−5]. Ni−Co electrodeposits due to higher toughness, strength and wear resistance are good replacement for conventional Ni deposits [6,7]. These improved properties arise from the role of cobalt in refining the microstructure and decreasing the necessity of addition of organic grain refiners [7]. Studies show that precipitation of C and N at grain boundaries, prevents the grain boundary sliding deformation mechanism and so limits the ductility and ultimate tensile strength (UTS) [7,8]. Application of these coatings specially at high temperatures promotes the precipitation of C, S and N, which leads to considerable reduction in mechanical properties [8]. Refining of microstructure by solid solution of Co element omits the brittleness and lowering of UTS resulted from organic grain refiner especially at high temperatures [6,7,9]. In this case, improving mechanical behavior makes the Ni−Co coatings applicable in anti-wear coatings and microsystems [10].

Ni−Co alloy coatings are electrodeposited from a diversity of simple and complex baths. Watts bath with addition of cobalt sulfate is one of the most commonly used baths [2,11−14]. It is worth noting that electroplating Ni−Co alloys are recognized as an anomalous co-deposition, i.e., higher adsorption ability of Co mono-hydroxide (e.g. $Co(OH)^+$) enriches the cobalt concentration in alloy coatings [1,15−19]. The amount of cobalt in Ni–Co coating can be controlled by process parameters, such as electrolyte composition, temperature, current density and pH [6,20,21]. Investigations show that the microstructure and properties of electrodeposited Ni−Co alloys forcefully depend on the cobalt content [2,6,20−25].

The knowledge of cobalt effect on deposition mechanism of these coatings will help us to better

**Corresponding author:** A. AMADEH; Tel: +98-21-82084609; Fax: +98-21-88006076; E-mail: amadeh@ut.ac.ir
DOI: 10.1016/S1003-6326(16)64136-5

control their microstructure and properties. Recently, electrochemical methods like cyclic voltammetry (CV) and electrochemical impedance spectroscopy (EIS) tests were successfully used as in-situ techniques to investigate the effect of additives on electrodeposition process [26−29]. The electrodeposition of Ni−Co film in various concentrations of cobalt was comprehensively studied by CV test [28]. However, the reports on EIS study of these coatings are rare. The EIS study of electrodeposition process of Ni−Co film can provide more information on electrodeposition mechanism with assistance of equivalent circuit which extends our knowledge about electrochemical deposition mechanism of these coatings.

On the other hand, several studies have been conducted on electrodeposition of Ni−Co coatings as well as investigation of their wear, corrosion and magnetic properties [2,21,30−35]. The performance of Ni−Co electrodeposits in anti-wear and microsystems applications is effectively dependent on their mechanical behavior. So, the investigation of tensile properties of these coatings will be beneficial.

In the present study, Ni–Co coatings were prepared from modified Watts bath. The electrodeposition mechanism, composition, morphology, crystallographic texture, hardness and tensile properties of the coatings were investigated as a function of cobalt concentration.

## 2 Experimental

A modified Watts bath consisting of 300 g/L $NiSO_4·6H_2O$, 45 g/L $NiCl_2·6H_2O$ and 45 g/L $H_3BO_3$ was used as essential electroplating bath. Cobalt sulfate ($CoSO_4·7H_2O$) was also added to electroplating bath from 0 to 120 g/L to produce Ni−Co coatings. A pure nickel plate with dimensions of 50 mm × 20 mm × 3 mm was used as anode. The coatings were prepared using square pulsed current with 50% duty cycle, 10 Hz frequency and 10 A/dm$^2$ peak current density. The electroplating pH and temperature were fixed at 4.5 and 50 °C, respectively. The bath was stirred by a magnetic stirrer during plating time which endured about 3 h.

To investigate the effect of cobalt on the electrochemical aspects of Ni−Co film, EIS tests were performed at $CoSO_4·7H_2O$ concentrations of 0, 40 and 80 g/L in bath at −1000 mV versus Ag/AgCl reference electrode. The results of EIS were used to simulate the equivalent electrical circuit of electrodeposition process using *Z*-view software.

Vickers microhardness tests were carried out on the specimens using a load of 80 g, applied for 5 s. The tensile tests were conducted by a MTS machine with a low capacity load cell (200 kg maximum) at constant strain rate of $1\times10^{-3}$ s$^{-1}$. To have free-standing samples that could be machined into fitting specimens for uniaxial tension tests, an Al cathode with plating area dimensions of 50 mm × 20 mm was used. The final thickness of the coatings was about 100 μm. After deposition, the coatings were stripped away from the substrate and cut to the dog-bone shaped tensile test sample with 5 mm in gage length and 3 mm in width by electro-discharge machining and afterwards polished to a mirror-like finish surface. A typical tensile test specimen is shown in Fig. 1. The coating morphology and crystallographic structure were investigated by means of scanning electron microscopy (SEM, VegaTescan) and X-ray diffractometer (XRD, PhilipsX'pert pro), respectively. The mass fraction of cobalt in the alloy coating was measured by energy dispersive X-ray spectroscopy (EDS).

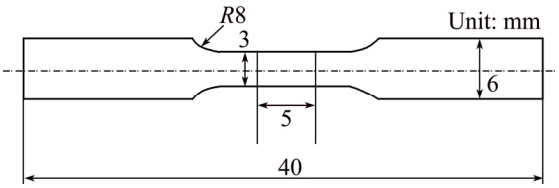


**Fig. 1** Typical schematic diagram of tensile test specimen

## 3 Results and discussion

### 3.1 EIS study of electroplating process

The Nyquist plots of EIS tests at different concentrations of cobalt in bath are shown in Fig. 2. The diagrams are composed of a high-frequency capacitive loop followed by a low-frequency inductive loop. Similar behavior was observed in deposition mechanism of Ni film in sulphamate bath [26]. It is believed that high-frequency capacitive loop is attributed to double layer capacitance and charge transfer resistance. The low frequency inductive loop is referred to adsorbed intermediates ions involved in electrodeposition process.

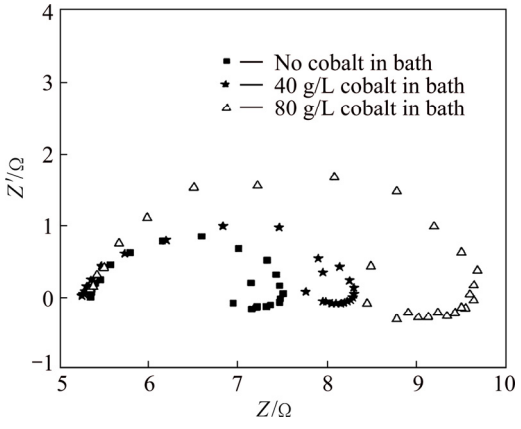


**Fig. 2** Nyquist plot of EIS results in Ni−Co deposition system at various concentrations of cobalt in bath at cathodic potential of −1000 mV (vs Ag/AgCl)

From Fig. 2, it is clearly seen that the cobalt concentration significantly affects both the high and low frequency loops. This indicates that the nature of electrical double layer as well as the adsorbed intermediate ions involved in electrodeposition process is changed in different cobalt concentrations in bath.

Some researchers [36,37] applied an inductive circuit (Fig. 3(a)) to describing the electrodeposition behavior, but some others [38] used a circuit that involves both a negative capacitor and a negative resistor (Fig. 3(b)). Due to the absence of appreciable magnetic field energy in front of the cathode, the second circuit provides more physical representation of the process leading to inductive features [38,39]. So, in present study, the equivalent circuit shown in Fig. 3(c) is used.

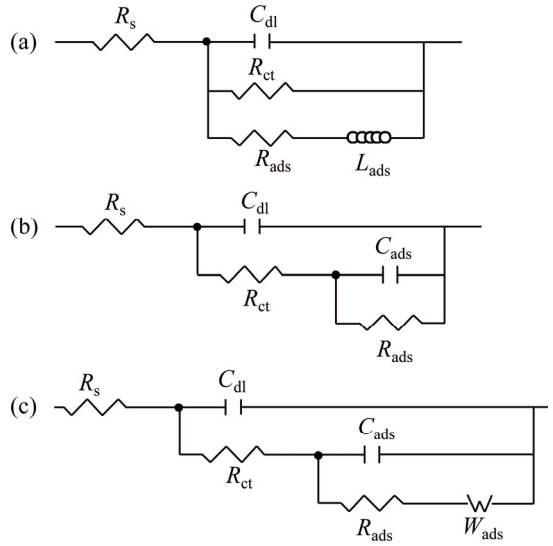


**Fig. 3** Equivalent circuit describing inductive behavior by inductive element (a), negative resistor and negative capacitor elements (b) and equivalent circuit (same as Fig. 3(b)) with addition of Warburg element (c)

In this circuit, $R_s$, $C_{dl}$, $R_{ct}$, $C_{ads}$ and $R_{ads}$ are the solution resistance, the double layer capacitance, the charge transfer resistance, pseudo-capacitance and pseudo-resistance of intermediates, respectively. $W_{ads}$ is the Warburg element incorporated in the circuit to account the effect of diffusional processes which are usually present in Ni−Co electrodeposition [27,40]. Table 1 summarizes the corresponding values of the elements used in equivalent circuit. It is clear that $R_{ct}$ values increase with increasing the Co concentration in bath, which indicates the increase in charge transfer formed on growing Ni−Co coatings. This may be related to the increase in adsorption of metal mono-hydroxides formed on cathode surface during electrodeposition. The mechanism proposed for electroplating of Ni−Co film is based on the formation and adsorption of metal hydroxyl ions on the deposits which can be expressed as follows [28]:

$$M^{2+}+OH^{-}=M(OH)^{+} \quad (1)$$

$$M(OH)^{+}\rightarrow M(OH)^{+}_{ads}(\text{electrostatic force of the cathode}) \quad (2)$$

$$M(OH)^{+}_{ads}+2e=M+OH^{-} \quad (3)$$

where M represents Co or Ni atom. It is possible that some of the adsorbed metal mono-hydroxide reacts with $OH^-$ ions and form metal hydroxides. Since the adsorption ability of cobalt mono-hydroxide ions is higher than that of nickel mono-hydroxide [28], increasing the Co ions can enhance the adsorption of Co ions. This can promote the formation of metal hydroxide on growing deposit and so increase the $R_{ct}$, since the presence of nonconductive metal hydroxide particles on cathode surface decreases the active surface and so increases the charge transfer.

In addition, it is clear that the increase in Co concentration in bath decreases the Warburg resistance. This shows that diffusion rate of the ions involved in electrodeposition process is enhanced by increasing the cobalt concentration. These ions are metal or metal mono-hydroxide ions which incorporate in the formation of metal deposit. Studies show that the deposition of Ni and Co ions in electrodeposition of Ni−Co coatings has activation and diffusional controlling rate, respectively [6]. An increase in Co concentration in bath, increases potential force for mass transport of $Co^{2+}$ or $Co(OH)^+$ ions towards the cathode. This can provide more number of metal or metal mono-hydroxide ions for electrodeposition process, which leads to a decrease in Warburg resistance.

### 3.2 Morphology and texture

The surface morphologies of the coatings are presented in Fig. 4. The cobalt contents of the deposits obtained from EDS analysis are also depicted in Fig. 5. The morphology of pure nickel deposit showing relatively large pyramidal grains is presented in Fig. 4(a).

**Table 1** Impedance parameters in Ni−Co deposition system at different concentrations of $CoSO_4·7H_2O$ in bath

| $\rho(CoSO_4·7H_2O)$/ ($g·L^{-1}$) | $R_s$/ ($\Omega·cm^{-2}$) | $C_{dl}$/ ($F·cm^{-2}$) | $R_{ct}$/ ($\Omega·cm^{-2}$) | $C_{ads}$/ ($F·cm^{-2}$) | $R_{ads}$/ ($\Omega·cm^{-2}$) | $W_{ads}$/ ($\Omega·cm^{-2}$) |
|---|---|---|---|---|---|---|
| 0 | 5.2 | $8\times10^{-4}$ | 7.7 | $-5\times10^{-4}$ | $-4\times10^{-2}$ | −9.5 |
| 40 | 5.1 | $21\times10^{-4}$ | 8.43 | $-8\times10^{-4}$ | $-2\times10^{-3}$ | −3.7 |
| 80 | 5.1 | $25\times10^{-4}$ | 10.14 | $-13\times10^{-4}$ | $-1\times10^{-2}$ | −1.7 |

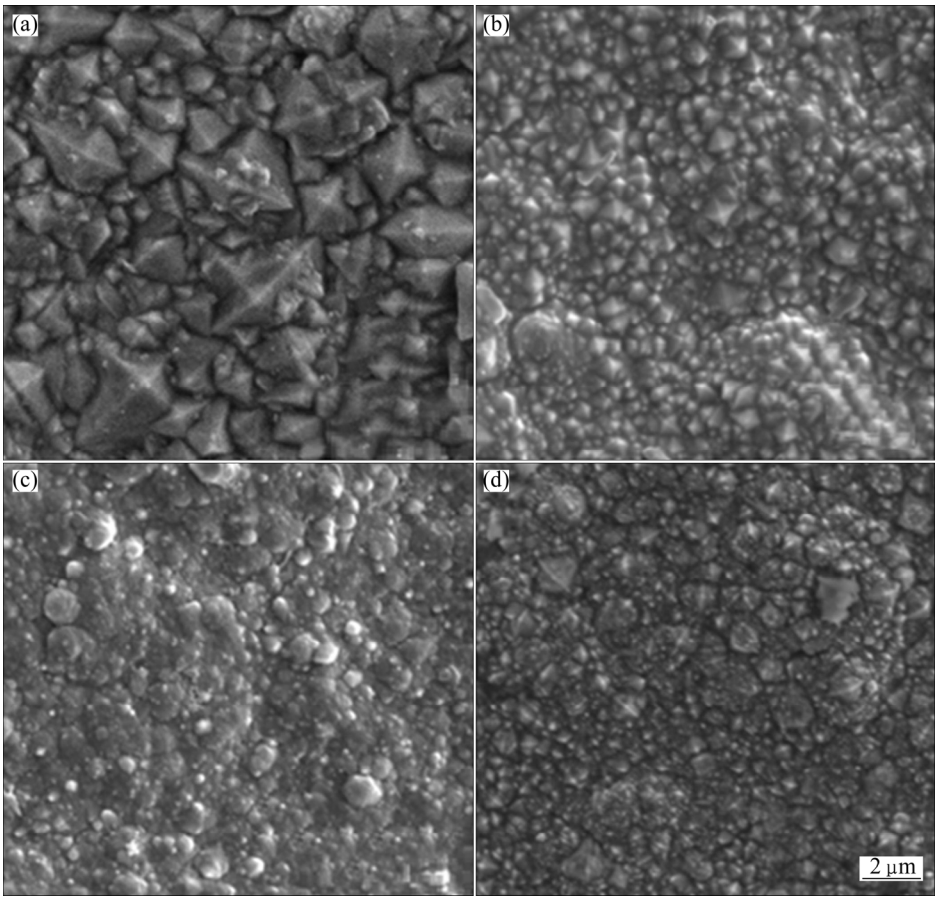


**Fig. 4** SEM images showing surface morphologies of Ni–Co deposits at various concentrations of cobalt sulfate: (a) 0 g/L; (b) 40 g/L; (c) 80 g/L; (d) 120 g/L

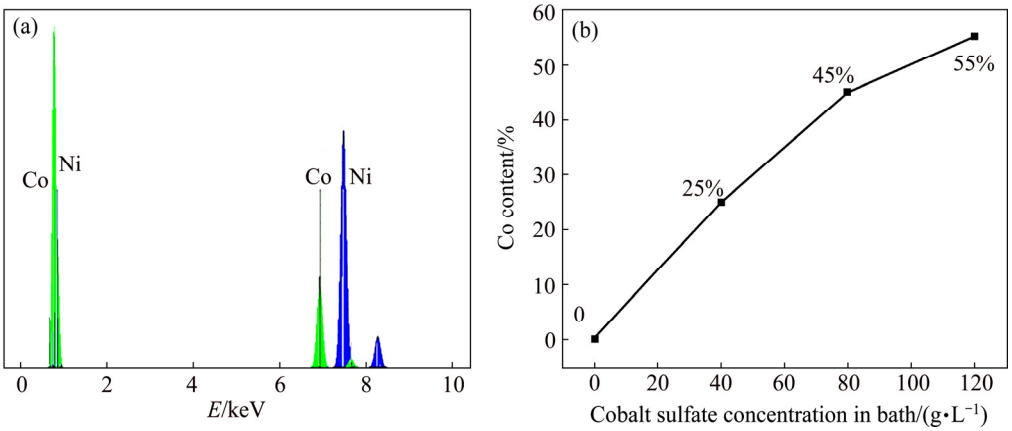


**Fig. 5** EDS spectrum of Ni−25%Co coating (a) and relationship between cobalt content and cobalt sulfate concentration in bath (b)

By increasing the cobalt content up to 45% (Figs. 4(b) and (c)), not only the grain size decreases but also the grain shapes change from pyramidal to spherical. This matter could be related to the influence of cobalt and nickel hydroxides on nucleation and growth mechanism. In Ni–Co alloy deposition, the absorbed $Ni(OH)^+$ and $Co(OH)^+$ mono-hydroxides are thought to block the growth centers of Ni and Co species during the off-time period, which retains their diffusion and leads to a decrease in growth rate of grains [41]. Figure 4(d) demonstrates light increment in size of grains at 55% of cobalt.

It is obvious from Fig. 5(b) that with increasing the cobalt ion concentration in electrolyte, cobalt content in coatings increases gradually. Furthermore, it can be seen that mass fraction of cobalt in coating is always more than the concentration of $Co^{2+}$ ions in electrolyte. This indicates the anomalous behavior of Ni−Co alloy

coatings which is in agreement with previous researches [2,6]. There are various reasons describing this anomalous behavior such as the competition between adsorption of metal hydroxides or metal ions, the formation of metal hydroxyl and variation of pH near the deposit surface [42,43].

XRD patterns of the coatings are displayed in Fig. 6. It can be seen that pure Ni coating exhibits (200) preferential crystallographic orientation which can be associated with the large grain size of Ni deposit. By addition of cobalt sulfate into electroplating bath, the intensity of (111) texture increases substantially whereas the intensity of (200) texture dwindles, which is in accordance with other researches [6]. It has been shown that the texture of electrodeposits depends on surface energy of growing crystallographic planes [44], so the consolidation of (111) texture can be attributed to the effect of $Co^{2+}$ ions on surface energy of growing crystallographic planes.

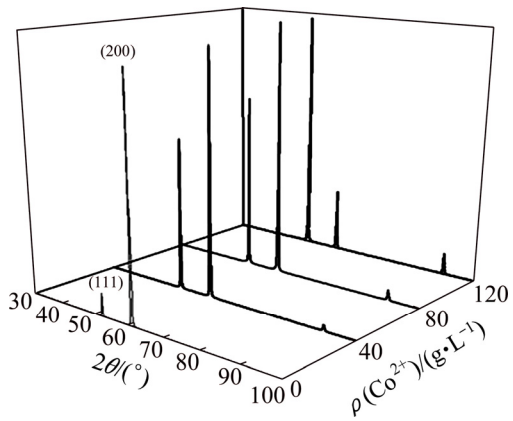


**Fig. 6** XRD patterns of Ni–Co deposits versus cobalt sulfate concentration

### 3.3 Mechanical behavior

True stress–true strain curves for pure Ni and Ni−Co alloy coatings with different contents of cobalt in coatings are illustrated in Fig. 7. To clarify the mechanical behavior of the coatings, their tensile strength and microhardness as a function of cobalt content are presented in Figs. 8(a) and (b). It is clear that up to 45% of cobalt, the hardness, yield strength ($\sigma_Y$) and ultimate tensile strength ($\sigma_{UTS}$) of the coating increase. It can be due to the decrease in grain size and solid solution strengthening of cobalt in the alloy coating. Moreover, the consolidation of (111) strong texture may be another reason for this increment. Commonly, strengthening polycrystalline metals and alloys by reduction in grain size is technologically noteworthy since it does not adversely affect the ductility and toughness [45]. It is also evident that when the cobalt content reaches 55%, the hardness, yield stress ($\sigma_Y$) and ultimate tensile strength ($\sigma_{UTS}$) decrease, compared with 45% of cobalt, which can be due to difference in the density of the coatings. It seems that Ni−45%Co coating is denser than Ni−55%Co one. In other words, the second coating contains more amounts of the defects such as voids and dislocations. The initial increment of ductility from 8.5% to 13.5% by increasing the cobalt content from 0 to 25% (Fig. 8(b)) in the coating can be attributed, on one hand,

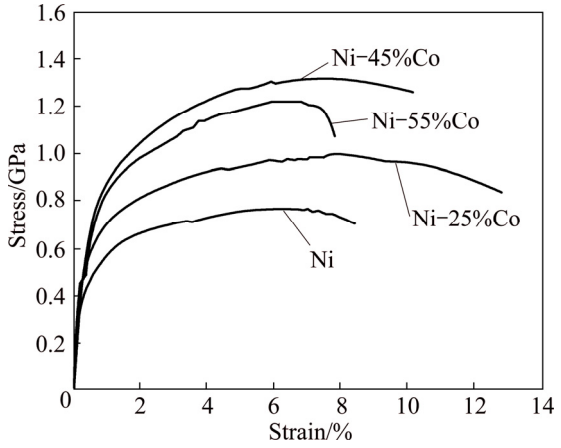


**Fig. 7** True stress–true strain curves of pure Co, pure Ni and Ni−Co deposits with different contents of cobalt

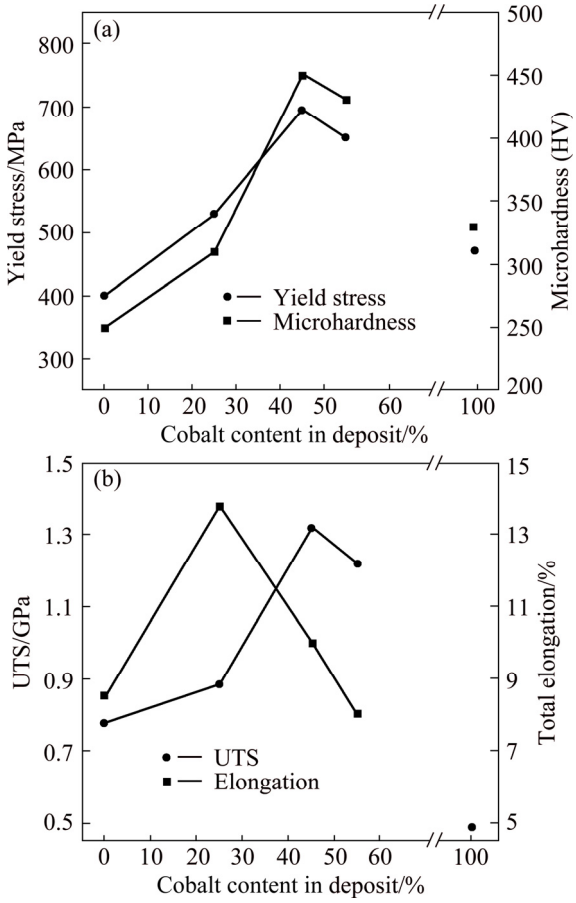


**Fig. 8** Microhardness and yield strength (a), elongation and ultimate tensile strength (b) of deposit as function of cobalt content (The elongation of pure cobalt is 0.2% and cannot be shown)

to the decrease in grain size. On the other hand, it was reported that for Ni−Co coatings, increasing the cobalt content up to about 20% leads to increase in the density of Ni−Co electrodeposits [2], which can be responsible for improving the ductility of the coatings. Increase in density of electrodeposits hinders the nucleation of voids and microcracks and so increases the ductility. Further increase in cobalt content (>25%) results in significant reduction of ductility, such that at 55% (Fig. 8(b)), the ductility reaches the lowest value.

It was reported that increase in cobalt content from 20% to 82% increases the porosity of Ni−Co deposits in Refs. [2,6]. The presence of porosity provides appropriate sites for nucleation of voids and microcracks and so decreases the ductility and promotes the fracture of electrodeposit. Moreover, it was shown that the increase in cobalt concentration promotes the deposition of metal hydroxides at grain boundaries [34], which can effectively decrease the ductility of electrodeposits.

SEM images of fractured surfaces of pure nickel and Ni−Co coatings with 25% and 55% of cobalt are illustrated in Fig. 9. As can be seen, all the samples show dimple fracture. The size of dimples in Ni−25%Co sample is smaller than that of pure Ni deposit. The decrease in dimple size with increase of cobalt content can be due to increment of prone sites for dimple formation such as grain boundaries and triple junctions. Also, at high stress values achieved in plastic deformation of Ni−25%Co deposit, more number of void–former sites are activated resulting in more number of dimples with lower size in comparison with pure Ni deposit [46]. In Fig. 9(c), many large voids can also be observed on fracture surface of Ni−55%Co electrodeposit, which are not the case for other coatings. These voids are probably the porosities produced during electrodeposition process at high cobalt concentrations. The presence of these porosities is effectively responsible for low ductility of Ni−55%Co deposits.

## 4 Conclusions

1) Increasing $Co^{2+}$ ions concentration in electroplating bath increased the charge transfer resistance and decreased Warburg impedance of growing Ni−Co layer, respectively.

2) With increasing $Co^{2+}$ ions in electroplating bath, cobalt content in the Ni−Co alloy coatings increased anomalously and (111) strong texture was improved progressively.

3) Addition of cobalt content up to 45% resulted in decreasing the grain size of deposit.

4) With addition of cobalt content up to 45%, the hardness, yield strength and ultimate tensile strength increased, whereas at 55% of cobalt these parameters decreased.

5) Maximum ductility was observed for Ni−25%Co coating. The micrographs of fracture surfaces indicated smaller dimples for this coating compared with other coatings.

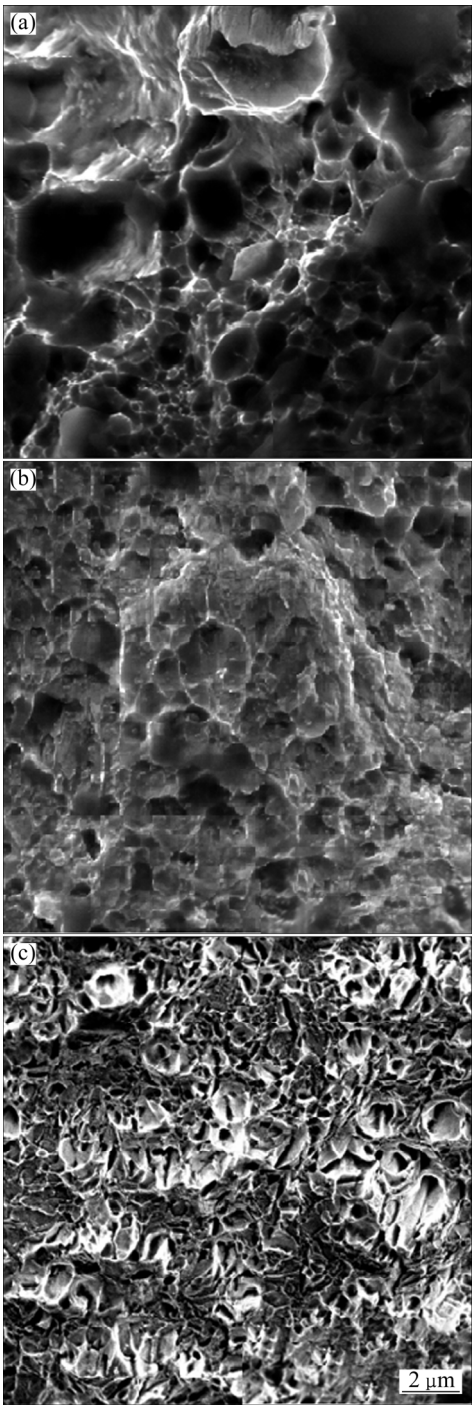


**Fig. 9** SEM image showing fractured surface micrographs of Ni (a), Ni−25%Co (b) and Ni−55%Co (c)

## References

[1] SAHOO P, DAS K. Tribology of electroless nickel coatings—A review [J]. Material & Design, 2011, 32(4): 1760−1775.

[2] SRIVASTAVA M, EZHIL SELVI V, WILLIAM GRIPS V K,

RAJAM K S. Corrosion resistance and microstructure of electrodeposited nickel–cobalt alloy coatings [J]. Surface and Coatings Technology, 2006, 201(6): 3051−3060.

[3] HU C C, WENG C Y. Hydrogen evolving activity on nickel–molybdenum deposits using experimental strategies [J]. Journal of Applied Electrochemistry, 2000, 30(4): 499−506.

[4] LUO J K, PRITSCHOW M, FLEWITT A J, SPEARING S M, FLECK N A, MILNE W I. Effects of process conditions on properties of electroplated ni thin films for microsystem applications [J]. Journal of Electrochemical Society, 2006, 153(10): 155−161.

[5] MC GEOUGH J A, LEU M, RAJURKA K P, SILVA A K M, LIU Q. Electroforming process and application to micro/macro manufacturing [J]. CIRP Annals−Manufacturing Technology, 2001, 50(2): 499−514.

[6] WANG Li-ping, GAO Yan, XUE Qun-ji, LIU Hui-wen, XU Tao. Microstructure and tribological properties of electrodeposited Ni−Co alloy deposits [J]. Applied Surface Science, 2005, 242(3): 326−332.

[7] LI Yun-dong, JIANG Hui, HUANG Wei-hua, TIAN Hui. Effects of peak current density on the mechanical properties of nanocrystalline Ni−Co alloys produced by pulse electrodeposition [J]. Applied Surface Science, 2008, 254(21): 6865−6869.

[8] YIN W M , WHANG S H, MIRSHAMS R A. Effect of interstitials on tensile strength and creep in nanostructured Ni [J]. Acta Materialia, 2005, 53(2): 383−392.

[9] FENINECHE N E, CODDET C, SAIDA A. Effect of electrodeposition parameters on the microstructure and mechanical properties of Co−Ni alloys [J]. Surface and Coating Technology, 1990, 41(1): 75−81.

[10] SHI Lei, SUN Chu-feng, GAO Ping, ZHOU Feng. LIU Wei-min. Mechanical properties and wear and corrosion resistance of electrodeposited Ni−Co/SiC nanocomposite coating [J]. Applied Surface Science, 2006, 252(10): 3591−3599.

[11] TURY B, RADNÓCZI G Z, RADNÓCZI G, VARSÁNYI M L. Microstructure properties of pulse plated Ni−Co alloy [J]. Surface and Coatings Technology, 2007, 202(2): 331−335.

[12] BURZYN´SKA L, RUDNIK E. The influence of electrolysis parameters on the composition and morphology of Co−Ni alloys [J]. Hydrometallurgy, 2000, 54(2−3): 133−149.

[13] BRENNER A. Electrodeposition of alloys [M]//Principles and Practice. Vol. II. London: Academic Press, 1963.

[14] LUPI C, DELL'ERA A, PASQUALI M, IMPERATORI P. Composition, morphology, structural aspects and electrochemical properties of Ni−Co alloy coatings [J]. Surface and Coatings Technology, 2011, 205(23−24): 5394−5399.

[15] CHUNG C K, CHANG W T. Effect of pulse frequency and current density on anomalous composition and nanomechanical property of electrodeposited Ni−Co films [J]. Thin Solid Films, 2009, 517(17): 4800−4804.

[16] KAKUNO E M, MOSCA D H, MAZZARO I, MATTOSO N, SCHREINER W H, GOMES M A B, CANTAO M P. Structure, composition and morphology of electrodeposited $Co_xFe_{1-x}$ alloys [J]. Journal of Electrochemical Society, 1997, 144(9): 3222−3226.

[17] LIN Yu-po, ROBERT SELMAN J. Electrodeposition of corrosion-resistant Ni−Zn alloy. I: Cyclic voltammetric [J]. Journal of Electrochemical Society, 1993, 140(5): 1299−1303.

[18] QIAO Gui-ying, JING Tian-fu, WANG Nan, GAO Yu-wei, ZHAO Xin, ZHOU Ji-feng, WANG Wei. High-speed jet electrodeposition and microstructure of nanocrystalline Ni−Co alloys [J]. Electrochimica Acta, 2005, 51(1): 85−92.

[19] VAES J, FRANSAER J, CELIS J P. The role of metal hydroxides in NiFe deposition [J]. Journal of Electrochemical Society, 2000, 147(10): 3718−3724.

[20] CORREIA A N, MACHADO S A S. Electrodeposition and characterisation of thin layers of Ni−Co alloys obtained from dilute chloride baths [J]. Electrochimica Acta, 2000, 45(11): 1733−1740.

[21] GOLODNITSKY D, ROSENBERG Y U, ULUS A. The role of anion additives in the electrodeposition of nickel–cobalt alloys from sulfamate electrolyte [J]. Electrochimica Acta, 2002, 47(17): 2707−2714.

[22] WANG C L, CHAN K C. Enhanced low-temperature superplasticity of Ni−Co alloy by addition of nano-$Si_3Ni_4$ particles [J]. Material Science and Engineering A, 2008, 491(1−2): 266−269.

[23] QIN L Y, LIAN J S, JIANG Q. Enhanced ductility of high-strength electrodeposited nanocrystalline Ni−Co alloy with fine grain size [J]. Journal of Alloys and Compounds, 2010, 504(S): s439−s442.

[24] GU C D, LIAN J S, JIANG Z H. High strength nanocrystalline Ni−Co alloy with enhanced tensile ductility [J]. Advanced Engineering Materials, 2006, 8(4): 252−256.

[25] GU C D, LIAN J S, JIANG Q. Ductile-brittle-ductile transition in an electrodeposited 13 nanometer grain sized Ni−8.6 wt.% Co alloy [J]. Materials Science and Engineering A, 2007, 459(1−2): 75−81.

[26] BENEA L D, LUIGI BONORA P, BORELLO A, MARTELLI S, WENGERE F, PONTHIAUXE P, GALLAND J. Preparation and investigation of nanostructured SiC–nickel layers by electrodeposition [J]. Solid State Ionics, 2002, 151(1−4): 89−95.

[27] FARZANEH M A, ZAMANZAD-GHAVIDEL M R, RAEISSI K, GOLOZAR M A, SAATCHI A, KABI S. Effects of Co and W alloying elements on the electrodeposition aspects and properties of nanocrystalline Ni alloy coatings [J]. Applied Surface Science, 2011, 257(13): 5919−5926.

[28] HU F, CHAN K C. Deposition behaviour and morphology of Ni−SiC electrocomposites under triangular waveform [J]. Applied Surface Science, 2005, 243(1−4): 251−258.

[29] RUDNIK E, BURZYN'SKA L, JĘDRUCH J, BŁAZ L. Codeposition of SiC particles with electrolytic cobalt in the presence of $Cs^+$ ions [J]. Applied Surface Science, 2009, 255(16): 7164−7171.

[30] PANDAY S, DANIEL B S S, JEEVANANDAM P. Synthesis of nanocrystalline Co−Ni alloys by precursor approach and studies on their magnetic properties [J]. Journal of Magnetism and Magnetic Materials, 2011, 323(17): 2271−2280.

[31] KEFALAS J H. Effect of electroplating parameters on magnetic properties of Ni−Co alloys [J]. Journal of Applied Physics, 1966, 37(3): 1160−1161.

[32] CHANG L M, AN M Z, SHI S Y. Corrosion behavior of electrodeposited Ni−Co alloy coatings under the presence of NaCl deposit at 800 °C [J]. Materials Chemistry and Physics, 2005, 94(1): 125−130.

[33] YANG Xiao-kui, LI Qing, ZHANG Shi-yan, GAO Hui, LUO Fei, DAI Yan. Electrochemical corrosion behaviors and corrosion protection properties of Ni−Co alloy coating prepared on sintered NdFeB permanent magnet [J]. Journal of Solid State Electrochemistry, 2010, 14(9): 1601−1608.

[34] TIAN Liang-liang, XU Jin-cheng, QIANG Cheng-wen. The electrodeposition behaviors and magnetic properties of Ni−Co films [J]. Applied Surface Science, 2011, 257(10): 4689−4694.

[35] SHI L, SUN C F, ZHOU F, LIU W M. Electrodeposited nickel–cobalt composite coating containing nano-sized $Si_3N_4$ [J]. Material Science and Engineering A, 2005, 397(1−2): 190−194.

[36] WATSON S W, WALTERS R P. The effect of chromium particles on nickel electrodeposition [J]. Journal of Electrochemical Society, 1991, 138(12): 3633−3637.

[37] WATSON S W. Electrochemical study of SiC particle occlusion during nickel electrodeposition [J]. Journal of Electrochemical Society, 1993, 140(8): 2235−2238.

[38] FRANCESCHETTI D R, MACDONALD J R. Electrode-kinetics, equivalent circuits, and system characterization-small-single-conditions [J]. Journal of Electroanalytical Chemistry, 1977, 82: 271−301.

[39] HU F, CHAN K C. Equivalent circuit modelling of Ni−SiC electrodeposition under ramp-up and ramp-down waveforms [J]. Materials Chemistry and Physics, 2006, 99(2−3): 424−430.
[40] BAI A, HU C C. Effects of electroplating variables on the composition and morphology of nickel-cobalt deposits plated through means of cyclic voltammetry [J]. Electrochimica Acta, 2002, 47(21): 3447−3456.
[41] TURY B, LAKATOS-VARSÁNYI M, ROY S. Ni−Co alloys plated by pulse currents [J]. Surface and Coatings Technology, 2006, 200(24): 6713−6717.
[42] GOLODNITSKY D, GUDIN N V, VOLYANUK G A. Study of nickel–cobalt alloy electrodeposition from a sulfamate electrolyte with different anion additives [J]. Journal of Electrochemistry, 2000, 147(11): 4156−4163.
[43] ZECH N, POKLAHA E J, LANDOLT D. Anomalous codeposition of iron group metals [J]. Journal of Electrochemistry, 1999, 146(8): 2886−2891.
[44] CHEN Li, WANG Li-ping, ZENG Zhi-xiang, XU Tao. Influence of pulse frequency on the microstructure and wear resistance of electrodeposited Ni−$Al_2O_3$ composite coatings [J]. Surface and Coatings Technology, 2006, 201(3): 599−605.
[45] ARZT E. Size effects in materials due to microstructural and dimensional constraints: A comparative review [J]. Acta Materialia, 1998, 46(16): 5611−5626.
[46] LARI BAGHAL S M, AMADEH A, HEYDARZADEH SOHI M, HADAVI S M M. The effect of SDS surfactant on tensile properties of electrodeposited Ni−Co/SiC nano–composites [J]. Materials Science and Engineering A, 2013, 559: 583−590.

# 钴含量对电沉积镍–钴合金电沉积机理和力学性能的影响

M. ZAMANI[1], A. AMADEH[1], S. M. LARI BAGHAL[1,2]

1. School of Metallurgy and Materials Engineering, College of Engineering, University of Tehran, P.O. Box 11155-4563, Tehran, Iran;
2. Department of Materials Science and Engineering, Faculty of Engineering, Shahid Chamran University, Ahvaz 6135785311, Iran

**摘　要**：在改进的 Watts 槽中电沉积不同钴含量镍−钴合金涂层，采用电化学阻抗谱方法研究钴含量对涂层电沉积机理的影响。采用 SEM 和 XRD 表征涂层的表面形貌和晶体结构。采用维氏显微硬度和拉伸试验确定涂层的力学性能。结果表明，随着电解槽中 $Co^{2+}$离子的增加，镍−钴涂层电荷转移电阻增加，相反 Warburg 阻抗降低。这可能是因为 $Co(OH)_2$ 阴极表面覆盖范围增大和金属离子向阳极表明扩散速率较高。而且，随着槽中钴含量的增加，合金涂层中的钴含量异常增加，(111)织构逐渐加强。当合金涂层的钴含量增加到 45%时，晶粒尺寸减小，随之合金的硬度和强度增大。进一步增加钴含量达 55%，合金的硬度和强度稍微降低。在 Ni−25%Co 涂层中能观察到最大的延展性，这是因为合金具有小晶粒尺寸和致密结构。

**关键词**：镍−钴涂层；电沉积；显微组织；力学性能

**(Edited by Xiang-qun LI)**